

Investigating core axial power distribution with multi-concentration gadolinium in PWR

Jing-Gang Li^{1,*} Jing-Han Peng¹ Chao Wang¹ Jun Chen¹ Fei Xu¹ Yun-Fan Ma¹

¹China Nuclear Power Technology Research Institute, Shenzhen 518000, China

*Corresponding author, lijinggang@cgnpc.com.cn

Abstract: Core axial power distribution is an essential topic in pressurized water reactor (PWR) reactivity control. Traditional PWRs limit stability against axial core power oscillations at a high-cycle burnup. Because the “camel” peak power shape typically occurs with increasing depletion, the approaches used for the axial power control deserve special attention. This study aims to investigate the performance of different gadolinium rod design schemes in core axial power control during power operation based on the reactivity balance strategy, and to propose new multi-concentration gadolinium rod design schemes. In the new design schemes, low-concentration gadolinium pellets are filled in the axial hump part of the gadolinium rod, and high-concentration gadolinium pellets are filled in the other parts. The impact of different gadolinium rod design schemes on the main core characteristics was evaluated using the nuclear design code package PCM developed by CGN. The results show that the new gadolinium rod design significantly impacts the core axial power shape. The new design schemes can efficiently improve the core axial power distribution along the entire cycle by reducing the core axial power peak at the end of a cycle, enhancing the reactor operation stability, and achieving a better core safety margin, revealing a sizeable potential application.

Key words: Gadolinium; PCM software package; Fuel assembly; Core axial power distribution; Reactivity

1. Introduction

Long-cycle fuel management is widely applied in current pressurized water reactor (PWR) designs to improve economic performance. For instance, most CGN CPR1000 reactors in China have applied 18-month fuel management instead of 12-month fuel management, which improves the annual power generation and introduces economic and social benefits. However, long-cycle fuel management requires higher critical boron concentrations at the beginning of cycle (BOC), which results in uneven power distributions. To reduce the boron concentration and flatten the power distribution, burnable poison rods were loaded into the fuel assembly.

Adding gadolinium is a mature burnable poison design with good performance, which has been proven in nuclear power plants worldwide. Multiple studies have focused on gadolinium burnable poison and long-cycle refueling. Asou and Porta studied the neutronics behavior of different

burnable poisons and presented a potential way to use gadolinium burnable poisons ^[1]. Huang et al. studied the progress of the burnable poison process and analyzed the properties of different burnable poisons ^[2]. Frybortova studied the limitations of burnable absorbers used in VVER fuel assemblies and concluded that gadolinium has the most significant influence on fuel characteristics ^[3]. Vnukov et al. analyzed the effects of gadolinium arrangement on the neutronic performance of a VVER-1200 fuel assembly ^[4]. Tran et al. investigated the neutronics design of a VVER-1000 fuel assembly with particles of gadolinium burnable poison ^[5]. Huang et al. studied the selection of both integrated- and separated-type burnable poisons for long-cycle reactor cores, and suggested enhancing the performance of long-cycle cores through proper matching of burnable poisons with low and high burnup rates ^[6]. Yang and Wu applied different optimization methods for in-core burnable poison loading in PWRs ^[7]. Xia et al. analyzed the burnup characteristics of a homogeneous mixing burnable poison for PWRs ^[8]. Xian et al. analyzed the different concentrations of gadolinium that impact the in-core fuel management for an 18-month PWR reload cycle ^[9]. Zhang et al. studied fuel management with gadolinium in an 18-month fuel cycle and quarter-core refueling for different nuclear power stations ^[10, 11]. Bai et al. analyzed the first startup physics test for a nuclear power plant loaded with gadolinium ^[12]. Galahom investigated the effect of gadolinium burnable absorbers on the neutronic characteristics of a PWR assembly over a very long cycle ^[13]. Mustafa and Amin studied the effect of gadolinium distribution on the neutronic parameters of a small modular reactor assembly ^[14]. Reda et al. investigated the performance and safety features of PWR using gadolinium poison from the Vera core physics benchmark ^[15]. Bejmer and Seveborn studied enriched gadolinium as a burnable absorber for PWRs ^[16]. Hu et al. used gadolinium as part of the backup reactivity in a 400 MW pool-type low-temperature heating reactor core ^[17].

At the BOC, the axial burnup distribution in the fresh fuel assembly is uniform, and the axial relative power in the middle is generally higher than that at the ends. As the fuel burnup increases, the power peaks gradually move towards the ends and form the "camel peaks" at high-cycle burnup. As the primary approach to adjusting the core axial power shape in the core, the control rods are implemented at the top of the vessel such that only one of the two "camel peaks" can be effectively restricted. Consequently, axial power perturbation can easily lead to divergent axial power oscillations. This phenomenon poses a challenge for axial power control and enforces the

heterogeneity power peak factor, which restricts the load following capacity and operational flexibility, particularly for reactors applying long-period refueling strategies.

Several studies have focused on the core axial power distribution of gadolinium. Owing to the significantly different axial power shapes at different cycle burnups, it is challenging for the fuel and core designs to control the power shape during the entire fuel cycle. Drumm et al. studied the optimal axial distribution of gadolinium in a PWR based on the Pontryagin maximum principle using the conjugate gradient method ^[18]. Hida et al. developed a method to optimize the axial enrichment and gadolinium distribution of boiling water reactor fuel to minimize the enrichment requirement ^[19]. Li et al. studied the core power capability of a core stretched-out operation and analyzed the core axial power distribution at different burnups ^[20]. Zhao et al. studied the core axial power distribution using a 3-D core power capability methodology ^[21]. Ma et al. studied the long cycle and low leakage loading technique for the first cycle and equilibrium cycle of HPR1000 with gadolinium and proposed a method to optimize the core axial power shape by replacing the gadolinium pellets at the ends with uranium pellets ^[22, 23]. Saad et al. performed a comparative analysis of fuels with different gadolinium axial distributions in the advanced PWR core. They proposed a core configuration in which gadolinium fuel rods were divided into three parts, with gadolinium fuel pellets in the central region ^[24].

In summary, the common idea to improve the core axial power shape is to replace a part of the uranium and gadolinium pellets. This study proposes a new method to improve the core axial power shape by adjusting the axial distribution of Gd_2O_3 concentration according to the reactivity rates. Pellets with low Gd_2O_3 concentrations are placed at the ends of the fresh fuel where the "camel peaks" occur, while the traditional gadolinium pellets are placed in other parts. The results show that this method significantly dampens the axial power "camel peaks", improves the core axial power distribution, and enhances operational flexibility.

2. Computer code

To analyze the impact of the gadolinium rod design in the core, a neutronic code system should be used to perform assembly/full-core neutronics analysis. There are alternatives such as CASMO/SIMULATE ^[17] and Serpent/PARCS ^[25]. This study uses the nuclear design code package

PCM developed by the CGN for analysis and calculation. The PCM code package consists of lattice code PINE and core code COCO.

PINE is mainly used to perform 2-D transport-depletion calculation on fuel assembly/assemblies and to generate the equivalent homogenized parameters of fuel assemblies and reflectors required by coarse-mesh nodal analysis for the 3-D core code COCO. The equivalent homogenized parameters include: 1) neutron diffusion coefficient; 2) average macro cross-sections of various types of assemblies; and 3) assembly surface discontinuity factors.

A 69-group cross-section library issued by the IAEA WLUP was adopted in PINE. The library consists of 175 nuclides and materials. This includes 23 actinides and 72 fission products. A detailed burnup chain of gadolinium is included in the library. The kinetic parameters of PINE were developed from JENDL4.0. The MOC method was applied for the 2-D heterogeneous transport calculation. The CMFD technique is used to accelerate the MOC solver. The B1 approximation model was used to correct the neutron spectra of the assembly, which were calculated under reflective boundary conditions. Two prediction-correction calculation methods, the LR method and LLR method, were applied in the depletion calculation of PINE. The code uses the LR method for fuel rods without gadolinium and applies the LLR method for fuel rods containing gadolinium to accelerate the calculation of gadolinium.

COCO was used to perform analyses such as reloading and reshuffling, depletion calculation, criticality search, control rod worth calculation, calibration curve calculation, and xenon transient calculation. It is a 3-D core code that uses the two-group assembly parameters generated by the lattice code PINE to perform neutron diffusion calculations. A non-linear iterative semi-analytical nodal method was adopted to solve the diffusion equation. The code depletion module includes both macroscopic and microscopic burnup calculations. The macroscopic burnup calculation deals with the burnup distribution in the core and the microscopic burnup calculation deals with the isotopic concentrations. The microscopic depletion module solves the depletion equation to obtain the concentration of each isotope at each burnup step. The neutron reactions analyzed in COCO include capture and induced fission reactions. The α decay and β decay reactions were adopted in the code. Isotopes analyzed by COCO include ^{154}Gd , ^{155}Gd , ^{156}Gd , ^{157}Gd , and ^{158}Gd . With the microscopic depletion module, COCO can accurately simulate the burnup behavior of gadolinium.

Many testing, verification, and validation studies have been conducted for the PCM code package to ensure calculation precision in PWR design [26–30]. The JAEA benchmark, criticality experiments, and operation data of CGN NPPs with gadolinium are used to validate the gadolinium calculation function of PCM. The verification and validation results show that the PCM code package has high accuracy in the gadolinium module and can be used to analyze gadolinium behavior.

This study uses PINE to analyze the fuel assembly reactivity change with burnup for different gadolinium schemes and COCO to study the core neutronic characteristics and power distribution loaded with gadolinium rods.

3. Gadolinium burnable poison reactivity analysis

There are seven gadolinium isotopes in nature: ^{152}Gd , ^{154}Gd , ^{155}Gd , ^{156}Gd , ^{157}Gd , ^{158}Gd , and ^{160}Gd . The most important isotopes for neutron absorption are ^{155}Gd and ^{157}Gd , as they have large neutron absorption cross-sections and account for an important natural share. In addition, although their neutron absorption cross-sections are not large, ^{154}Gd and ^{156}Gd have a relatively significant share in nature. After absorbing neutrons, these two isotopes become ^{155}Gd and ^{157}Gd , and special attention should be paid to their analysis.

Because of the excellent neutron absorption properties mentioned above, gadolinium is widely used as a burnable poison in reactor design to control core reactivity and flatten the power distribution. During manufacturing, the gadolinium burnable poison is in the powder form after being homogeneously mixed with Gd_2O_3 and UO_2 and sintered into gadolinium pellets. Compared with UO_2 pellets, gadolinium pellets have a lower thermal conductivity and lower melting point. Therefore, in the reactor design, to ensure gadolinium rod integrity, the ^{235}U enrichment in the gadolinium pellets was lower than that in the uranium pellet, and the Gd_2O_3 concentration in the gadolinium pellet was limited to $\leq 10\%$. The ^{235}U enrichment in gadolinium pellets (θ), concentration of Gd_2O_3 in gadolinium pellets (μ), and ^{235}U enrichment in uranium pellets (ε) in a fuel assembly generally need to satisfy the following criteria:

$$\theta \leq \varepsilon - c\mu \quad (1)$$

where, c is a constant.

Owing to the strong neutron absorption ability of gadolinium, thermal neutrons are quickly absorbed when passing through the outer layer of the gadolinium pellet, and it is difficult to penetrate the outer layer to reach the inner layer of the gadolinium pellet, resulting in a noticeable spatial self-shielding effect. This space self-shielding effect is considered in detail in PINE when calculating the reactivity characteristics of the gadolinium burnable poison.

Traditional gadolinium burnable poison generally adopts an integral arrangement. Several gadolinium rods were placed in the fuel assembly and gadolinium pellets were loaded into the gadolinium rods. This design has no constraints on the loading pattern. Gadolinium rods were mixed with the fuel rods. Theoretically, the gadolinium pellets can be placed anywhere in the fuel assembly. The axial and radial distribution of gadolinium pellet concentrations can be changed arbitrarily. Compared with other burnable poisons such as IFBA and WABA, the gadolinium burnable poison provides more extensive design flexibility. For instance, the 12 ft 17×17 fuel assembly consisted of 264 fuel rods. Each fuel rod contained a fixed number of fuel pellets. A certain number of gadolinium rods ^[17] can be flexibly placed in the fuel assembly. Two typical layouts with 8 and 24 gadolinium rods in the fuel assembly are shown in Fig. 1.

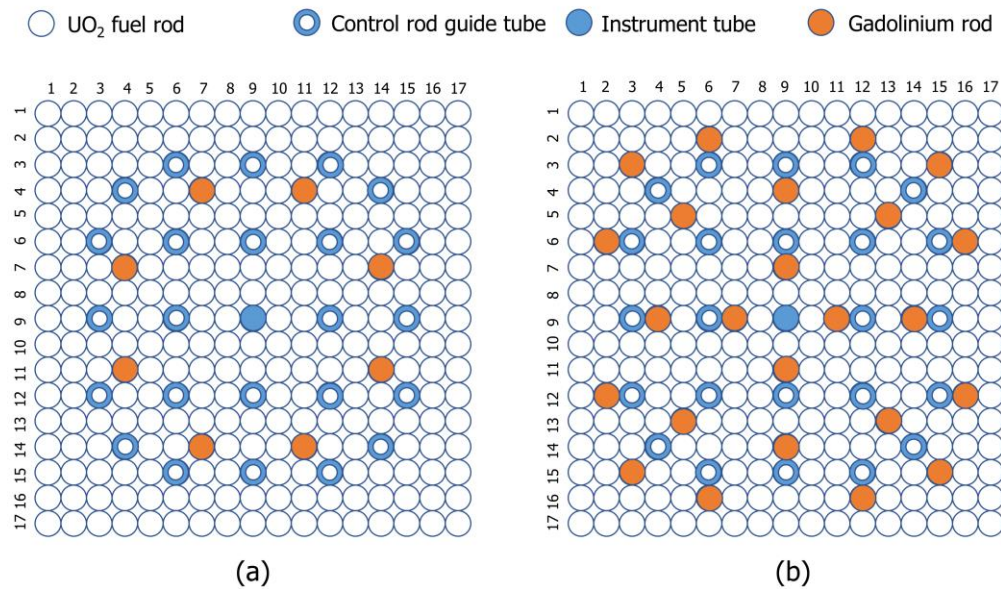


Fig. 1 (Color online) Gadolinium rod layout in fuel assemblies. (a) Assembly with 8 Gd-rods. (b) Assembly with 24 Gd-rods.

The number of gadolinium rods has a significant influence on fuel assembly reactivity. Fig. 2a shows the infinite multiplication factor (k_{inf}) curves of fuel assemblies with different numbers of gadolinium rods. The initial ^{235}U enrichment in the UO_2 pellets was set to 4.45 wt%, the initial ^{235}U enrichment in the gadolinium pellets was set to 2.5 wt%, and the initial Gd_2O_3 concentration was set to 8%. Figure 2a shows that the fuel assembly with more gadolinium rods had a lower initial reactivity. Fuel assemblies with different gadolinium rods have the same inflection point of burnup and reactivity decline rate after the inflection point.

The Gd_2O_3 concentration in the pellets also has a significant impact on fuel assembly reactivity. Fig. 2b shows the k_{inf} curves of fuel assemblies with different Gd_2O_3 concentrations. The initial ^{235}U enrichment in the UO_2 pellets was set to 4.45 wt%, the initial ^{235}U enrichment in the gadolinium pellets was set to 2.5 wt%, and the number of gadolinium rods was set to 24. Fig. 2b shows that the fuel assembly with lower Gd_2O_3 concentrations had a higher initial reactivity with the same gadolinium rods. The reactivity peak during burnup and the burnup inflection point for the fuel assembly differed with the Gd_2O_3 concentration. The fuel assembly with a lower Gd_2O_3 concentration had a higher reactivity peak during burnup and reached its peak earlier. The fuel assembly with a higher Gd_2O_3 concentration had a lower reactivity peak during burnup and reached a peak later. After the reactivity peaks, the fuel assemblies with different Gd_2O_3 concentrations exhibit the same reactivity decline rate.

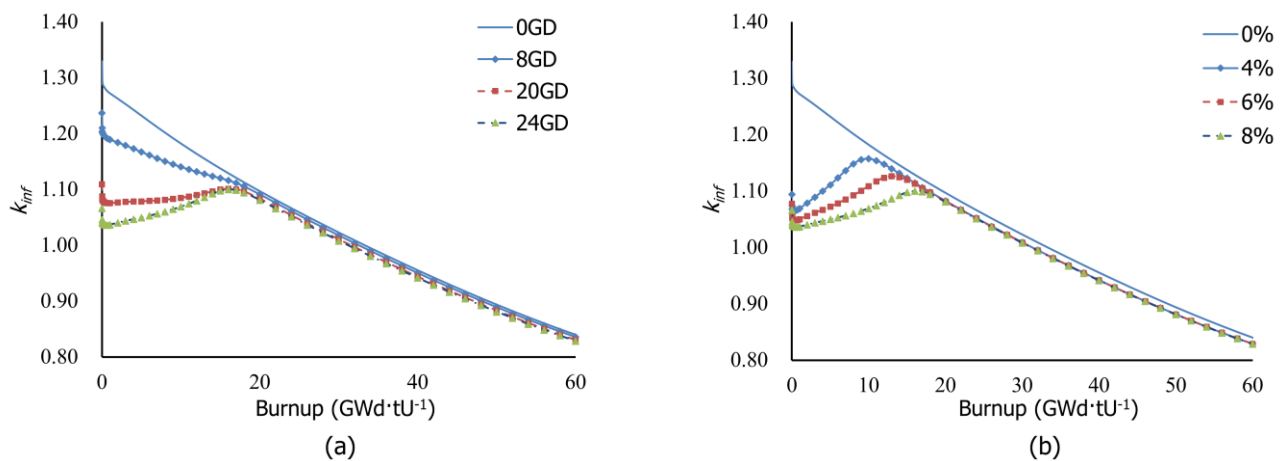


Fig. 2 (Color online) Fuel assembly k_{inf} variation versus burnup. (a) With different numbers of gadolinium rods. (b) With different Gd_2O_3 concentration.

Figure 2 shows that there is a specific reactivity penalty for gadolinium burnable poison in the later stages of burnup. The reactivity penalty of the gadolinium burnable poison in the later stage of burnup increases with the number of gadolinium rods and Gd_2O_3 concentration. This characteristic of gadolinium burnable poison must be comprehensively considered when designing the reactor core.

4. New gadolinium rod design scheme

The design of the gadolinium burnable poison is mainly associated with the optimization of four parameters: 1) the Gd_2O_3 concentration in the gadolinium pellet; 2) the ^{235}U enrichment of the gadolinium pellet; 3) the number of gadolinium rods per assembly; and 4) the location of the gadolinium rods in the assembly.

In the traditional fuel assembly design, to simplify the fuel assembly manufacturing process, the fresh fuel pellets in one fuel rod are typically kept the same for the entire axial height, as well as the gadolinium pellets (see "Traditional design" in Fig. 3a).

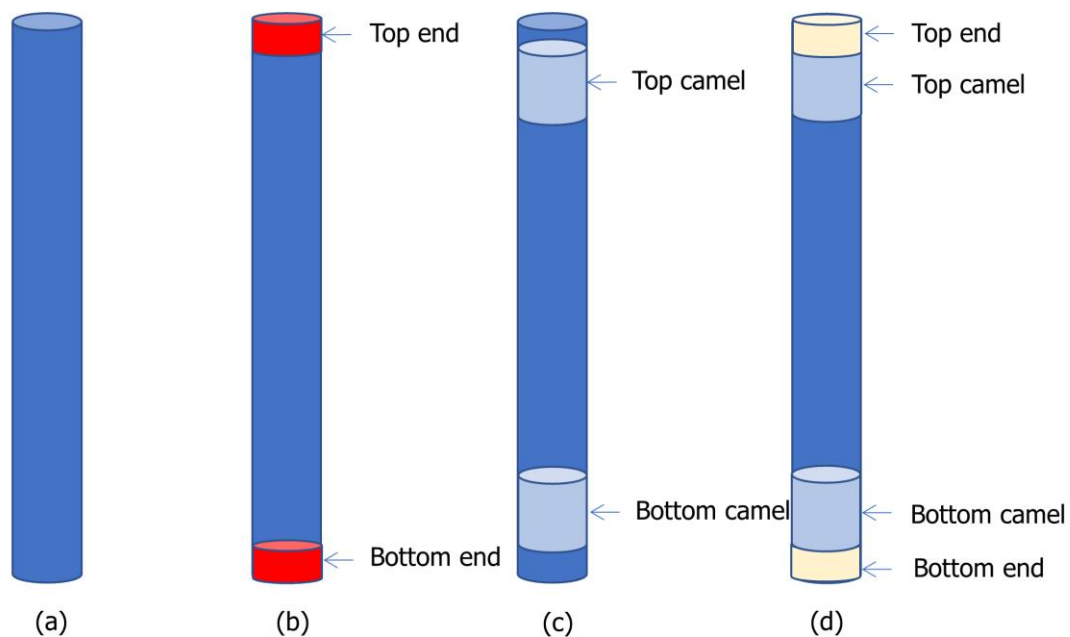


Fig. 3 (Color online) Pellet axial layout in gadolinium rod. (a) Traditional design. (b) Modified design. (c) New design-I. (d) New design-II.

Although the number of gadolinium rods in the fuel assembly is limited (typically only accounting for $<1/10$ of the fuel assembly), because of its good neutron absorption characteristics,

gadolinium significantly affects the radial and axial power distribution of the core. To optimize the radial power distribution of the core, gadolinium rods are typically arranged near the position of the guide tube in the fuel assembly (as shown in Fig. 1) to reduce the fuel rod power caused by better neutron moderation. Simultaneously, with in-depth research on gadolinium burnable poisons, the axial design of gadolinium rods has been continuously improved to optimize the core axial power distribution. One of the modified designs involves loading uranium pellets with identical ^{235}U enrichment in the same fuel assembly at both ends of the gadolinium rod (see "Modified design" in Fig. 3b), in which the core axial power distribution is improved by the replacement of gadolinium and UO_2 pellets [21–22].

As discussed in Sect. 3, the fuel assembly reactivity decline rate changes with different gadolinium concentrations. With the reactivity peak shifting strategy for different gadolinium concentrations, it is possible to flatten the axial power shape by releasing the local reactivity in the region where the "camel peaks" appear before the power peak.

Based on this strategy, in order to improve the axial power shape along the whole fuel cycle, mainly to flatten the "camel peaks" appearing at the end of cycle (EOC), this study proposes a new gadolinium rod design method with different concentration gadolinium pellets: the pellets with a low Gd_2O_3 concentration are placed where "camel peaks" appear and the pellets with a high Gd_2O_3 concentration are placed in other parts. Adopting this method, two new gadolinium rod arrangement schemes were designed in this study, as shown in Fig. 3c (New design-I) and Fig. 3d (New design-II). The main feature of the "New design-I" scheme is that the lower concentration gadolinium pellets are symmetrically arranged at the position where the "camel peaks" appear (the "Top Camel" and "Bottom Camel" region in Fig. 3c); the main feature of the "New design-II" scheme is that, in addition to placing low concentration gadolinium pellets at the hump region, lower Gd_2O_3 concentration gadolinium pellets are placed at the bottom and top of the core ("Bottom End" region and "Top End" region in Fig. 3d). The "New design-II" scheme comprehensively considers the various reactivity of different gadolinium burnable poison, and forms a certain gadolinium concentration gradient distribution from the hump to the ends.

Whether it is the "Modified design" scheme, "New design-I" scheme, or "New design-II" scheme, the new gadolinium rod design schemes take advantage of the flexibility of gadolinium

pellets in the axial arrangement of gadolinium rods, and there is no difficulty in fuel assembly manufacturing.

Compared to other gadolinium design schemes to improve the core axial power distribution (such as the "Modified design" scheme), there are two main characteristics of the new gadolinium design schemes in this study:

- 1) Gadolinium pellets with a low Gd₂O₃ concentration were adopted instead of UO₂ pellets in the standard way to replace the high Gd₂O₃ concentration gadolinium pellets, which permits precise adjustment of the axial power distribution.
- 2) Gadolinium pellets with a low Gd₂O₃ concentration were adopted in the hump regions instead of only in the top/bottom parts in the standard way, which permits local adjustment of the axial power distribution near the hump regions.

5. Influence on core characteristics

This study is based on the CGN PWR fleet CPR1000 with 18-month fuel management. There were 157 fuel assemblies with 4.45 wt% enrichment in the equilibrium cycle, including 72 fresh assemblies. Fresh assemblies included 8 or 20 gadolinium rods. The core thermal power was 2895 MW and the core average coolant temperature at full power was 310 °C. The "Mode G" load-following mode was adopted in the CPR1000. The main core characteristics at 100%NP of the CPR1000 are listed in Table 1.

Table 1 Main Core characteristics at 100%NP

Parameters	Value
Number of loops	3
Total heat output (MWth)	2905
Core heat output (MWth)	2895
Power density, kW/liter of core	107.2
Average linear power density at 100%NP (W/cm)	186.0
Total flow of pumps (m ³ /hr)	70116
Core flow rate in % total flow rate	93.5
Coolant pressure (bar)	155
Zero load inlet temperature (°C)	291.4
Inlet temperature at 100%NP (°C)	292.7
Core average coolant temperature at 100%NP (°C)	310.0

To analyze the influence of the new design scheme on the core characteristics, the related parameters of each gadolinium rod design scheme in Fig. 3 are as follows:

- 1) Traditional design scheme (Fig. 3a): the Gd_2O_3 concentration of the gadolinium pellets was uniformly set to 8%.
- 2) Modified design scheme (Fig. 3b): the Gd_2O_3 concentration of gadolinium pellets in the main part was set to 8%, and the "Top End" and "Bottom End" parts in Fig. 3b used 4.45 wt% ^{235}U enrichment uranium pellets.
- 3) New design-I scheme (Fig. 3c): the Gd_2O_3 concentration of gadolinium pellets at the "Top Camel" and "Bottom Camel" in Fig. 3c was set to 6%, and the remainder used gadolinium pellets with a Gd_2O_3 concentration of 8%;
- 4) New design-II scheme (Fig. 3d): gadolinium pellets with a Gd_2O_3 concentration of 6% were used for the "Top Camel" and "Bottom Camel" in Fig. 3d. From the hump to the ends of the gadolinium rod ("Top End" and "Bottom End" in Fig. 3d), gadolinium pellets with a Gd_2O_3 concentration of 4% were used, and gadolinium pellets with a Gd_2O_3 concentration of 8% were used for the remainder.

The ^{235}U enrichment in all gadolinium pellets was set to 2.5%. In this study, all the new assemblies loaded in the core used only one specific gadolinium rod design scheme among the four mentioned schemes. A combination of gadolinium rod design schemes was not considered.

In the original design of the CPR1000 18-month fuel management, the core of the equilibrium cycle is loaded with fresh assemblies containing gadolinium rods of the "Traditional design" scheme in Fig. 3a. In this study, the gadolinium rods in the fresh assemblies were replaced by the design schemes shown in Fig. 3b, 3c, and 3d. The quarter-core loading pattern for this equilibrium cycle is shown in Fig. 4a. All other features in the fuel and core designs are the same for all of these schemes.

Table 2 shows a comparison of the main core neutronic parameters such as the critical boron concentration (C_B), moderator temperature coefficient (MTC), and Doppler temperature coefficient (DTC) under the conditions of BOC, hot zero power, and all control rods out. The C_B for the four schemes were similar, and the MTC and DTC were negative, all of which met the design requirements.

Table 2 Core neutronics parameters

Scheme	C_B (ppm)	MTC (pcm/°C)	DTC (pcm/°C)
Traditional design	1934	-4.76	-3.23

Modified design	2013	-1.77	-3.23
New design-I	1944	-4.27	-3.24
New design-II	1975	-3.40	-3.25

The core boron letdown curves for different design schemes are shown in Fig. 4b. It can be seen that the trends of the boron concentration along the entire cycle for the different schemes are similar. This is readily understandable because the local design changes of the gadolinium rods in the new fuel assembly have little effect on the total reactivity of the core.

The impact of different design schemes on radial power distribution was further investigated. The variation in the core radial power peak factor ($F_{\Delta H}$) with the burnup at full power is shown in Fig. 4c. All $F_{\Delta H}$ values for the different schemes satisfy the design requirement. However, as shown in Fig. 4c, compared with the other schemes, the "Modified design" scheme has the lowest $F_{\Delta H}$ and the most flattened radial power during the whole cycle. The $F_{\Delta H}$ of the "New design-I" scheme is close to the "Traditional design" scheme at the BOC, but slightly larger than the "Traditional design" scheme at the gadolinium peak burnup. The $F_{\Delta H}$ of the "New design-II" scheme is similar to that of the "Traditional design" scheme throughout the cycle.

Figure 4d highlights the effects of different design schemes on the core axial power offset (AO) with burnup. Figure 4d shows that the four design schemes have similar characteristics of AO variation with cycle burnup: at the BOC, AO is relatively positive; as the fuel depletes, AO gradually becomes negative and reaches a negative absolute maximum value; then, the variation trend of AO reverses, AO gradually becomes positive with fuel depletion and reaches a positive maximum value, and finally, AO gradually decreases until the EOC. The complex change in AO with burnup is mainly determined by the non-linear variation in the reactivity of gadolinium-containing fuel assemblies with burnup. In addition, compared with the "Traditional design" scheme, the other three gadolinium rod design schemes have a slightly larger maximum AO value at the gadolinium peak burnup. Although the AO of these three new design schemes can still meet the operational needs, special attention should be paid to this phenomenon in nuclear design.

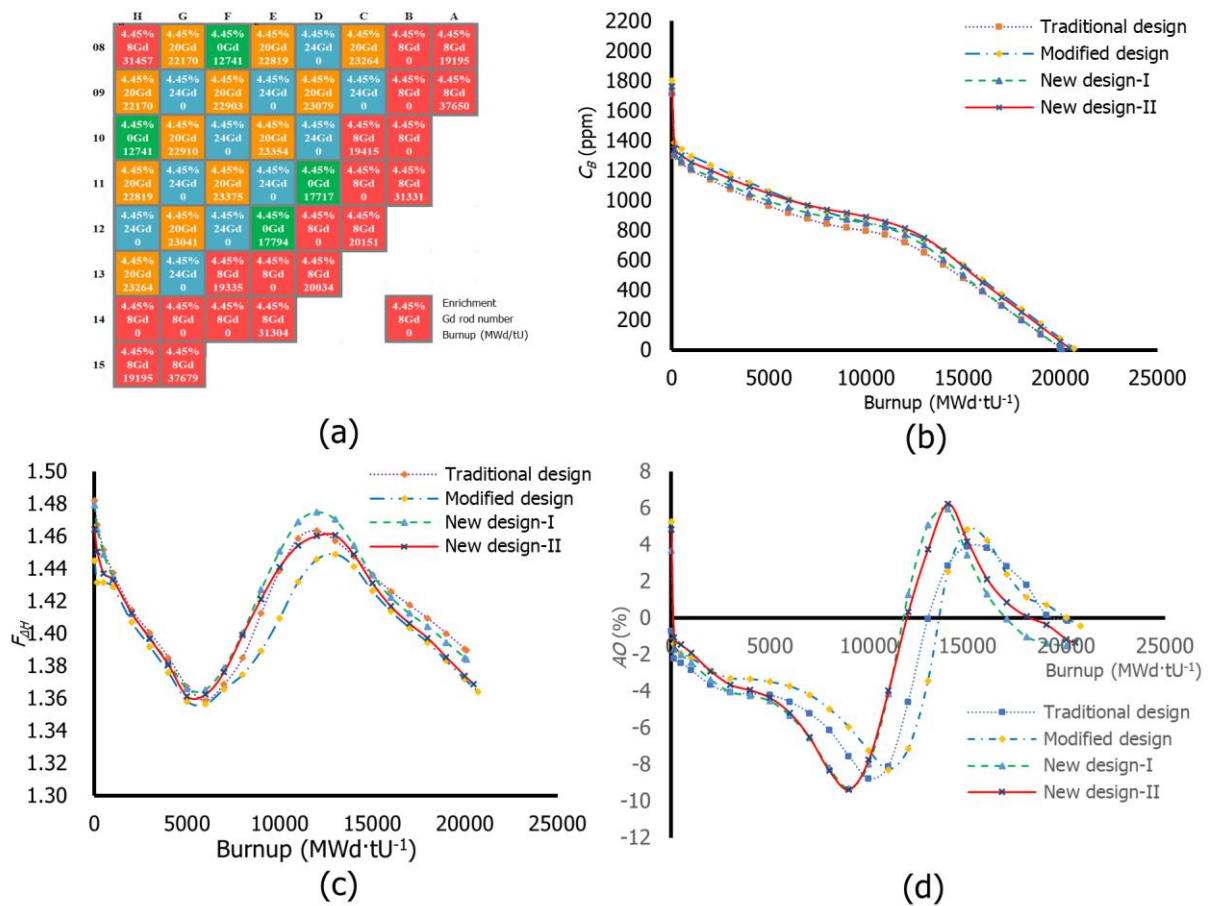


Fig. 4. (Color online) Main core parameters (a) Core reshuffling pattern. (b) Boron letdown curve. (c) F_{AH} variation. (d) AO variation.

Furthermore, this study investigated the effects of different design schemes on the core axial power distribution in more detail. Figure 5 shows a comparison of the core axial power distribution (P_z) under full-power steady-state conditions for different cycle burnups. In general, with the increase of cycle burnup, the core axial power is increasingly concentrated at both ends, and the axial power shape gradually shifts from "olive" to "camel". Simultaneously, the core axial power distribution of the different schemes shows individual features with burnup.

- 1) For the "Modified design": compared with the "Traditional design" scheme, because of the use of UO_2 pellets at the ends of the gadolinium rod, the core axial power at the top and bottom ends was relatively high at the BOC. With fuel depletion, it gradually evolved into a hump-shaped power distribution.
- 2) For the "New design-I": the gadolinium pellets at the "Top Camel" and "Bottom Camel" regions were replaced with lower Gd_2O_3 concentration pellets. Compared with the "Traditional design",

the local reactivity at the hump regions were slightly higher at the BOC, which was conducive to flattening the "olive" core axial power distribution at this moment. As the cycle burnup increased, owing to the low Gd_2O_3 concentration in the hump regions, the reactivity decreased faster than in other regions. This design scheme is beneficial for flattening the hump-shaped power distribution at a later stage of the cycle.

- 3) For the "New design-II": based on "New design-I", gadolinium pellets with lower Gd_2O_3 concentration were additionally used at the top and bottom ends of the gadolinium rod. Therefore, compared with "New design-I", the core axial power shape of this scheme was more inclined to the upper and lower ends of the core, which was conducive for better flattening of the "olive" power distribution at the BOC. Because the gadolinium pellets with lower Gd_2O_3 concentration at the ends had faster reactivity consumption, it was beneficial to reduce the reactivity at the hump regions with the burnup increase. Therefore, "New design-II" was better than "New design-I" in optimizing the core axial power shape throughout the entire cycle, reaching a level equivalent to the "Modified design".

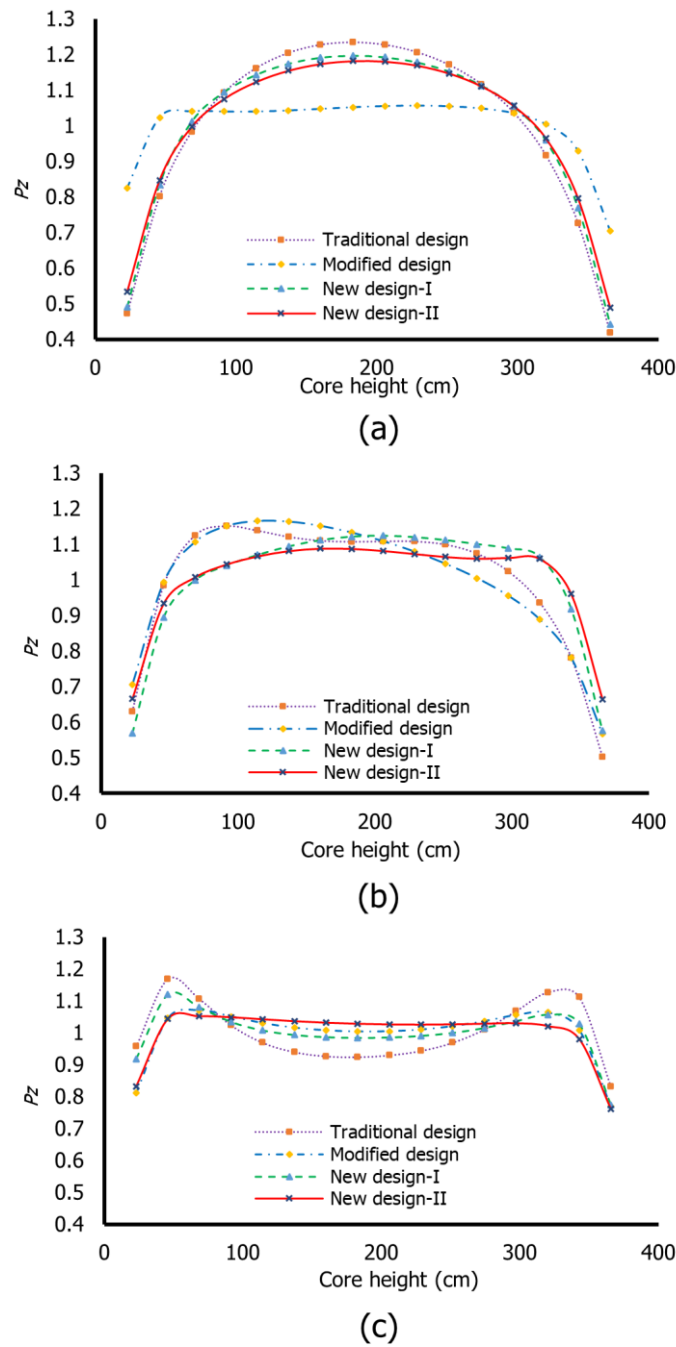


Fig.5 (Color online) Axial power distribution variation versus core height. (a) BOC. (b) MOC. (c) EOC.

In general, whether at the beginning, middle or end of the cycle, compared with "Traditional design", "Modified design" and "New design-II" have a better effect on improving core axial power shape, while the effect of "New design-I" design is less important.

Compared with "Traditional design", the other three schemes reduce the local power at the hump regions of the core at the later stage of the cycle, which is beneficial to control the core xenon transient and reduce the risk of xenon oscillations. Taking the xenon transient with a power

disturbance introduced into the reactor at the EOC as an example, the reactor power decreased from 100% FP to 95% FP instantaneously, and the reactor control system remained inactive. COCO was used to simulate the core behavior for 72 h using different gadolinium rod design schemes. Figure 6a and 6b show a comparison of the core axial power deviation (ΔI) and core power peak factor (F_q) under this xenon transient for the four schemes.

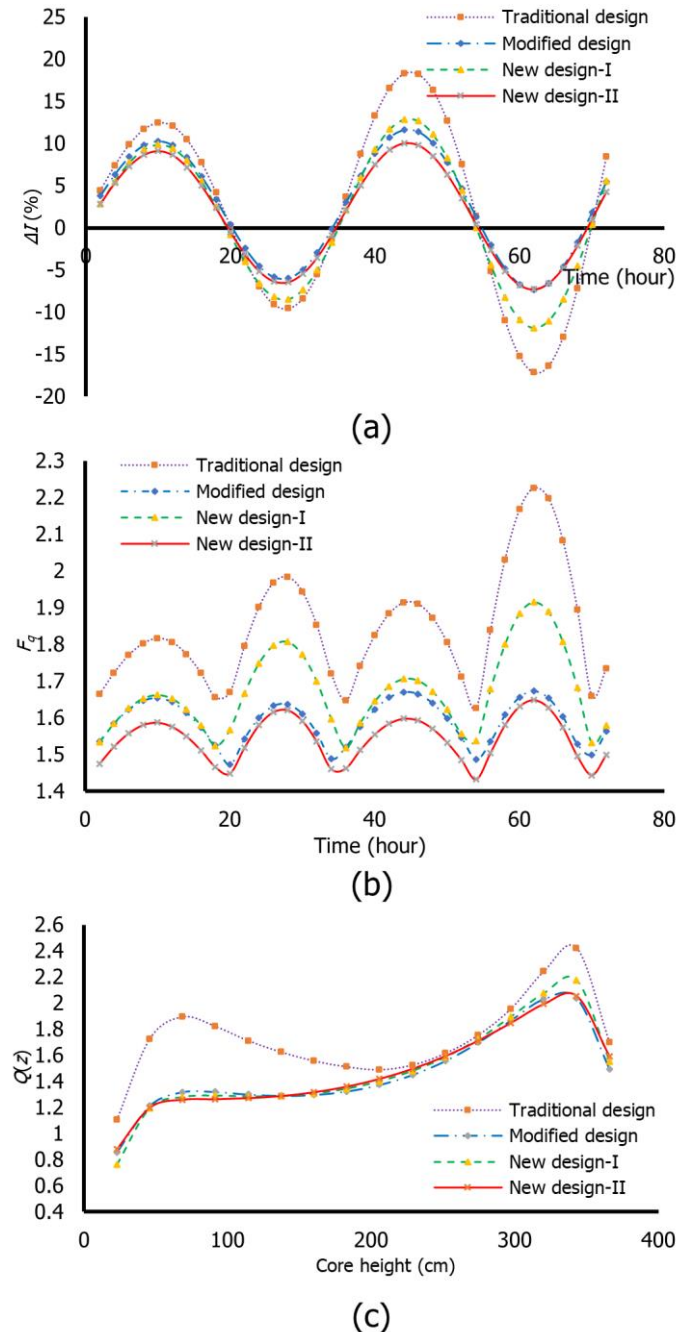


Fig.6 (Color online) Xenon transient simulation. (a) ΔI variation with time at EOC. (b) F_q variation with time at EOC. (c) Axial power peak shape under most penalizing condition.

Figure 6a shows that, in this xenon transient, ΔI tends to diverge gradually for the core using the "Traditional design" scheme; while for the core using the other three schemes, ΔI is relatively stable. The core of "New design-II" is the most stable in this transient, followed by "Modified design" and "New design-I."

Figure 6b shows that, in this xenon transient, the F_q of "Traditional design" has a significant uptrend, while the F_q of the other schemes is relatively stable and is significantly less than that of "Traditional design." "New design-II" has the lowest F_q in this transient, followed by "Modified design" and "New design-I".

Compared with "Traditional design," the other three schemes improve xenon transient control performance, which is beneficial to enhance the core load follow capability. Through a 3-D core power capability analysis of key penalizing states, this study evaluated the core power peaks under normal operating conditions. The axial power peak shape under the most penalizing conditions for these four schemes is shown in Fig. 6c. The results show that the other three schemes smoothen the axial power shape under transient conditions. F_q at this penalizing state of "Traditional design" was 2.41, while the F_q of "Modified design", "New design-I", and "New design-II" were 2.03, 2.16, and 2.04, respectively, which were reduced by 15%, 10%, and 15%, respectively, compared with "Traditional design." This evidence supports the idea that the new design schemes enhance the safety margin and have good application potential.

Therefore, "Modified design", "New design-I", and "New design-II" can significantly improve the core power shape, promote the control capability, and enhance the core safety margin.

6. Sensitivity analysis on gadolinium concentration

In the analysis in Sects. 4 and 5, the Gd_2O_3 concentration in the hump regions was set to 6%. However, according to Fig. 2, the reactivity behavior versus burnup is different for gadolinium pellets with different Gd_2O_3 concentrations. To analyze the characteristics of different Gd_2O_3 concentrations, this study performed a sensitivity analysis of the axial power shape with different Gd_2O_3 concentrations in the hump regions. The sensitivity study is based on "New design-II" and adopts a Gd_2O_3 concentration of 4% in the "Top Camel" and "Bottom Camel" regions.

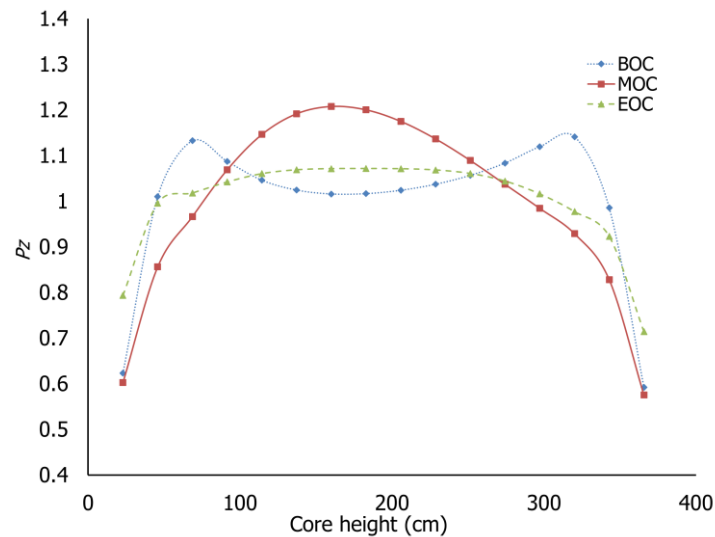


Fig.7 (Color online) Axial power distribution variation versus core height of sensitivity design

Figure 7 provides the core axial power distribution (P_z) of this sensitivity study at different cycle burnups. These curves show that the power shape has obviously different features from the design schemes in Sect. 5. For the sensitivity study scheme, the core occurs "camel" axial power shape at the BOC and gradually changes into an "olive" axial power shape with burnup. The initial reactivity is relatively greater for gadolinium pellets with 4% Gd_2O_3 concentration, which leads to higher local power in these regions. From the sensitivity analysis, we can conclude that the Gd_2O_3 concentration at the hump regions should be carefully designed with an appropriate concentration for the gadolinium pellets at the hump regions to balance the reactivity between the hump regions and other regions to improve the axial power shape for the entire cycle.

7. Conclusion and outlook

Traditional PWRs exhibit significant limits owing to the axial core power oscillation. The design of a gadolinium burnable poison can substantially affect the shape of the axial power of the core. To improve the axial power shape and dampen the axial camel peak power at the EOC, this study investigated four different gadolinium rod design schemes and compared their core characteristics. The PCM code package was used to analyze the fuel assembly characteristics and core behavior.

The analysis shows that these four design schemes have similar core characteristics in terms of $F_{\Delta H}$ and AO variation with cycle burnup. Compared with "Traditional design", "Modified design" uses ^{235}U uranium pellets at the ends of the gadolinium rod and has a good axial power shape along the whole cycle. "New design-I" places low Gd_2O_3 concentration pellets in the hump regions which

can decrease the core axial power peak to a certain degree. Based on "New design-I", "New design-II" adopts lower gadolinium concentration pellets at the ends of gadolinium rod and achieves a better effect than "New design-I". In general, these two new design schemes can efficiently improve the core axial power shape. Besides, "Modified design" and "New design-II" can reduce the core power peak factor by almost 15% compared with "Traditional design" under the transient conditions. "Modified design" and "New design-II" improve the core axial power shape most effectively, and significantly reduce the power peak factor in key transient states.

To improve the axial power shape for the entire cycle, the Gd_2O_3 concentration in the hump region should be carefully designed with an appropriate concentration to balance the reactivity between the hump regions and other regions.

All of these new design schemes require little cost and only a slight modification from the current design, but can significantly improve the core axial power distribution.

Therefore, these new design schemes of gadolinium rod can improve the core safety margin, enlarge the capability of load following and operational flexibility, and have good application prospects.

Although the new designs proposed in this study are beneficial, we believe that they can be extended and optimized. Among these possibilities are the following.

- 1) Implementing different concentrations of gadolinium pellets at the top and bottom hump regions instead of the same concentration may further benefit the core axial power shape.
- 2) Implementing higher concentrations of gadolinium pellets at different regions axially instead of focusing on the hump and end regions in the gadolinium rods may further benefit the core axial power shape.

Acknowledgments

We greatly appreciate the generous help of Dr. Qing Zhou who provided us with an instructive discussion.

Author contributions

All authors contributed to the study conception and design. Material preparation, data collection and analysis were performed by Jing-Gang Li, Jing-Han Peng, Chao Wang, Jun Chen, Fei Xu and Yun-Fan Ma. The first draft of the manuscript was written by Jing-Gang Li and all authors

commented on previous versions of the manuscript. All authors read and approved the final manuscript.

References

- 1 M. Asou, J. Porta, Prospects for poisoning reactor cores of the future. Nucl. Eng. Des. 168, 261-270 (1997). [https://doi.org/10.1016/S0029-5493\(96\)01322-2](https://doi.org/10.1016/S0029-5493(96)01322-2)
- 2 H. Huang X. Wang, J. Yang et al., Research on surface-modification of nanoparticles powder. Development and Application of Materials 04, 87-91 (2014) (in Chinese)
- 3 L. Frybortova, Recommended strategy and limitations of burnable absorbers used in VVER fuel assemblies. Nucl. Sci. Tech. 30, 129 (2019). <https://doi.org/10.1007/s41365-019-0651-x>
- 4 R.A. Vnukov, V.V. Kolesov, I.A. Zhavoronkova et al., Effect of the burnable absorber arrangement on the VVER-1200 fuel assembly neutronic performance. Nucl. Energy Technol. 7, 215-221 (2021). <https://doi.org/10.3897/nucet.7.73490>
- 5 H.N. Tran, V.K. Hoang, P.H. Liem et al., Neutronics design of VVER-1000 fuel assembly with burnable poison particles. Nucl. Eng. Technol. 51, 1729-1737 (2019). <https://doi.org/10.1016/j.net.2019.05.026>
- 6 S. Huang, P. Yang, L. Wang et al., Research on Selection of Burnable Poisons for Long-Life Reactor Core. Nuclear Power Engineering 38, 6-10 (2017). <https://doi.org/10.13832/j.jnpe.2017.02.0006> (in Chinese)
- 7 B. Yang, H. Wu, Optimization Calculation for In-Core Burnable Absorber Fuel Loading for Pressurized Water Reactor. Nuclear Power Engineering 26, 214-218 (2005) (in Chinese)
- 8 Y. Xia, S. Xu, J. Xie et al., The research on burnup characteristic of homogeneous Mixing Burnable Poison for PWR Rod Fuel Assembly. Journal of University of South China(Science and Technology) 34, 34-41 (2020). <https://doi.org/10.19431/j.cnki.1673-0062.2020.04.006> (in Chinese)
- 9 C. Xian, Z. Zhang, X. Liu et al., Burnable poison optimization study for mega-Kw PWR nuclear power plant long cycle core. Nuclear Power Engineering 20, 193-196 (1999) (in Chinese)
- 10 H. Zhang, L. Li, Q. Li et al., Fuel management study on 18 months fuel cycle for Daya Bay Nuclear Power Station. Nuclear Power Engineering 23, 14-17 (2002) (in Chinese)
- 11 H. Zhang, J. Li, Fuel management study on quarter core refueling for Ling Ai NPP. Nucl. Sci.

- Eng. 32, 85-92 (2012) (in Chinese)
- 12 C. Bai, L. Wang, X. Fu et al., Analysis for first startup physics test for unit 1 of Ningde Nuclear Power Plant. Nucl. Sci. Eng. 34, 332-336 (2014) (in Chinese)
 - 13 A.A. Galahom, Investigation of different burnable absorbers effects on the neutronic characteristics of PWR assembly. Ann. Nucl. Energy 94, 22-31 (2016).
<http://dx.doi.org/10.1016/j.anucene.2016.02.025>
 - 14 S.S. Mustafa, E.A. Amin, The effect of soluble boron and gadolinium distribution on neutronic parameters of small modular reactor assembly. Radiat. Phys. Chem. 171, 1-11 (2020).
<https://doi.org/10.1016/j.radphyschem.2020.108724>
 - 15 S.M. Reda, S.S. Mustafa, N.A. ELHawas, Investigating the performance and safety of Pressurized water reactors using the burnable poison. Ann. Nucl. Energy 141, 1-10 (2020).
<https://doi.org/10.1016/j.anucene.2020.107354>
 - 16 K.H. Bejmer, O. Seveborn, Enriched gadolinium as burnable absorber for pwr. La Grange Park: American Nuclear Society, Lagrange Park, IL, 25-29 (2004)
 - 17 B. Hu, X. Liu, Z. Sun et al, Nuclear design of 400 MW pool-type low-temperature heating reactor core. Nuclear Techniques 44, 100606 (2021) doi: 10.11889/j.0253-3219.2021.hjs.44.100606 (in Chinese)
 - 18 C.R. Drumm, J.C. Lee, Gadolinium burnable absorber optimization by the method of conjugate gradients. Nucl. Sci. Eng. 96, 17-29 (1987). <https://doi.org/10.13182/NSE87-1>
 - 19 K. Hida, R. Yoshioka, Optimization of axial enrichment and gadolinia distributions for BWR fuel under control rod programming, (II) optimization of reload fuel. J. Nucl. Sci. Technol. 29, 313-324 (1992). <https://doi.org/10.1080/18811248.1992.9731531>
 - 20 J. Li, H. Zhang, W. Liang et al., Study on core power capability during stretch-out for LingAo nuclear power station. Nuclear Power Engineering 26, 62-64 (2005) (in Chinese)
 - 21 C. Zhao, J. Wang, X. Fu et al., Optimization analysis of 3D core power capability verification. Nucl. Sci. Eng. 37, 1061-1065 (2017) (in Chinese)
 - 22 Z. Ma, J. Su, S. Zhou, Research of optimization technology for equilibrium cycle with gadolinium. Nuclear Power Engineering 42, 1-5 (2021) (in Chinese)
 - 23 Z. Ma, J. Su, S. Zhou, Study on the long cycle and low leakage loading technique for the first

- cycle with gadolinium. Nucl. Sci. Eng. 41, 290-297 (2021) (in Chinese)
- 24 H. Saad, R. Refeat, M. Aziz et al., Comparative analysis of fuel with different gadolinium axial distribution in advanced pressurized water reactor core. J. Nucl. Particle Phys. 12, 1-13 (2022).
<https://doi.org/10.5923/j.jnpp.20221201.01>
- 25 V.P. Tran, K.C. Nguyen, D. Hartanto et al., Development of a PARCS/Serpent model for neutronics analysis of the Dalat nuclear research reactor. Nucl. Sci. Tech 32, 15 (2021).
<https://doi.org/10.1007/s41365-021-00855-5>
- 26 H. Lu, K. Mo, W. Li et al., Development of self-reliant three-dimensional core nuclear design code COCO. Atomic Energy Science and Technology 47, 327-330 (2013) (in Chinese)
- 27 H. Lu, J. Chen, J. Wang et al., Verification and validation of self-reliant core nuclear design code COCO. Atomic Energy Science and Technology 51, 1460-1463 (2017) (in Chinese)
- 28 J. Li, C. Wang, J. Chen et al., Development and verification of fuel assembly bowing model in software package PCM. High Power Laser and Particle Beams 34, 026004 (2022) (in Chinese).
<https://doi.org/10.11884/HPLPB202234.210378>
- 29 CGN, PINE - A Lattice Physics Code: Verification and Validation Report,
GHX00600004DRDG02TR (2020)
- 30 CGN, COCO - A 3-D Nuclear Design Code: Verification and Validation Report,
GHX00600001DRDG02TR (2020)